

Article

Gluconic Acid Leaching of Spent Lithium-Ion Batteries as an Environmentally Friendly Approach to Achieve High Leaching Efficiencies in the Recycling of NMC Active Material

Reinhard Lerchbammer *, Eva Gerold and Helmut Antrekowitsch

Chair of Nonferrous Metallurgy, Montanuniversitaet Leoben, 8700 Leoben, Austria; eva.gerold@unileoben.ac.at (E.G.); helmut.antrekowitsch@unileoben.ac.at (H.A.)

* Correspondence: reinhard.lerchbammer@unileoben.ac.at; Tel.: +43-3842-402-5222

Abstract: Organic acids, such as gluconic acid, have been widely studied for their potential in the hydrometallurgical recycling of lithium-ion batteries. These organic alternative leachants offer several environmental and recycling-related benefits, including a high selectivity in terms of dissolving valuable metals, as well as a reduced environmental impact due to the application of non-toxic and biodegradable organic acids. Gluconic acid has previously been demonstrated in the oxidative degradation of glucose, either as an alternative reducing agent or in biometallurgical approaches, and has been described as an efficiency-supporting reagent. The results of this study demonstrate the effectiveness of using gluconic acid for the recovery of metals such as lithium, cobalt, nickel, and manganese from spent lithium-ion batteries. Recovery rates of above 98% for lithium, cobalt, and manganese, and a recovery rate of more than 80% for nickel could be reached by optimizing the leaching parameters, including an acid concentration of 1.2 M, the addition of hydrogen peroxide of 1.6 vol %, a solid-to-liquid ratio of 25 g/L, a leaching temperature of 75 °C, and a leaching time of 192 min. These results show that gluconic acid has the potential to become a viable and sustainable option for the hydrometallurgical recycling of lithium-ion batteries, as well as for opening a possible biohydrometallurgical route. Further investigations are required into the results obtained, to verify the existence of a new hydrometallurgical and sustainable process route involving gluconic acid.

Keywords: lithium-ion battery recycling; NMC black mass; hydrometallurgy



Citation: Lerchbammer, R.; Gerold, E.; Antrekowitsch, H. Gluconic Acid Leaching of Spent Lithium-Ion Batteries as an Environmentally Friendly Approach to Achieve High Leaching Efficiencies in the Recycling of NMC Active Material. *Metals* **2023**, *13*, 1330. <https://doi.org/10.3390/met13081330>

Academic Editors: Fernando Castro and Daniel Assumpcao Bertuol

Received: 19 June 2023
Revised: 24 July 2023
Accepted: 24 July 2023
Published: 25 July 2023



Copyright: © 2023 by the authors. Licensee MDPI, Basel, Switzerland. This article is an open access article distributed under the terms and conditions of the Creative Commons Attribution (CC BY) license (<https://creativecommons.org/licenses/by/4.0/>).

1. Introduction

Every year, the production capacity of lithium-ion batteries (LIBs) increases rapidly. Since the first lithium-ion battery was used in mobile applications, the market has been growing steadily. One reason for this is the political measures that must be taken due to the increase in greenhouse gases produced by the transport sector; within the European Union (EU-27) alone, the increase amounted to 110 million metric tons of CO₂-equivalent gases from 1990 to 2021. Without the contribution of international shipping and aviation, the transport sector is generally responsible for around 21% of the emissions recorded in the European Union, which is why it is in precisely this sector that an enormous difference can be made [1–4].

In particular, national strategies to achieve net-zero emissions have caused the sales of electric vehicles to soar to the level of 16.5 million units, as sold in 2021. In March 2023, the EU member states agreed to a ban on the sale of non-CO₂-neutral light vehicles and passenger cars from 2035 onward. These measures should help to reduce emissions and make Europe climate-neutral by 2050 [5–7].

In this context, it is important to discuss the European Green Deal program [8], which is intended to enable supplying the entire economy and society with sustainably produced energy. This requires innovative energy storage systems, with battery technologies being

explicitly mentioned in the proposal. Therefore, the EU is promoting new forms of governmental collaboration with industry. The European Commission will continue to implement the Strategic Action Plan for Batteries and support the European Battery Alliance. The aim is to establish frameworks for a complete, globally competitive, and sustainable battery value chain in the EU, which will ensure strategic independence in this sector. Such a value chain includes the assessment of recycling quotas to ensure that the residual materials from batteries are appropriately recycled. For lithium-ion batteries, the revision of the Battery Directive 2006/66/EG is important in this context. In addition to the prescribed collection quotas, this directive contains recycling efficiencies on both modular and elementary levels. As of 2030, 70% of lithium-ion batteries must be recycled on a modular basis. At the elemental level, it is mandatory that 95% of the elements Co, Ni, and Cu are to be recovered, and 70% of Li [8–10].

Moreover, the Critical Raw Materials Act [11] has been presented in parallel with the EU Net Zero Industry Act [12] by the European Union to improve resilience regarding supply shortages of critical raw materials. Besides ensuring additional secure and sustainable supply chains, recycling is a key factor for the critical strategic supply of technology-related metals. A variety of different materials and elements are incorporated into lithium-ion batteries. Some of these were already among the raw materials considered critical within the European Union in 2020. Lithium, cobalt, nickel, copper, and phosphorus, as well as phosphate rock and metallic silicon, are already classified as critical components, while other widely used elements, such as sulfur or iron, are considered of high economic importance [11–13].

In addition to these legal requirements, the recycling of lithium-ion batteries offers the possibility of taking batteries of all types and conditions—end-of-life, damaged, and rejected batteries, product residues, etc.—and processing them into new raw materials. The variety of material compositions and chemistries that are used in such products makes it challenging to establish a stable and universal recycling process. New developments with the aim of increasing reliability, energy, power density, service life, and safety, combined with cost-effective production, open up a wide range of material compositions that can be recycled in different ways. Knowledge of the materials used and their similarities is essential for designing effective recycling facilities and processes [2,14,15].

Increased prices for lithium carbonate, nickel, and cobalt, in addition to political measures and supply risks, open up the possibility of economically feasible processing for recovering the most valuable ingredients from LIBs. Previously, in 2019, Bernhart et al. [16] showed that, depending on recycling efficiency and the processing route, profits can be made from recycling. Figure 1 gives an insight into the price development of lithium carbonate, cobalt, nickel, manganese, copper, and aluminum in USD per ton for the period from 2016 to 2022 [16].

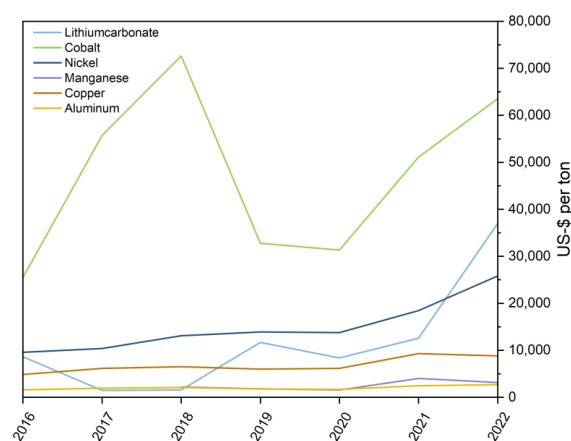


Figure 1. Price development of battery components for the period 2016 to 2022 (data from refs. [17–22]).

For a recycling or processing facility, there are stringent safety requirements due to the complex material compositions and high levels of halogen-containing and organic compounds, as well as the energetic content and the required efficiencies. Previous developments have led to the development of two process routes. The first route combined pyrometallurgy with hydrometallurgical treatment to recover valuable metals, i.e., copper, nickel, and cobalt. Depending on the process control, lithium can be found in the slag as well as in the off-gas products. Wet chemical methods are also required for the recovery of both manganese and lithium from the slag, along with lithium from the off-gas, and are currently the subject of research. When LIBs are used directly, the fly ash serves as a drain for undesirable by-elements, such as fluorine; therefore, it is subsequently landfilled. The second option operates only hydrometallurgically, requiring mechanical as well as thermal pretreatment. There is no universal process pathway that takes either pyro- or hydrometallurgical routes for spent lithium-ion batteries; therefore, both processes use a combination of different mechanical and thermal pretreatments [15,23–26].

The pretreatment of LIBs essentially involves discharging and thermal treatment, usually followed by pyrolysis to remove the organic and halogen compounds, and finally mechanical shredding. In addition, mechanical processing can remove the plastic components, as well as copper, aluminum, and steel before pyrolysis. The obtained product is called black mass and consists of the valuable and critical elements of carbon, lithium, nickel, cobalt, and manganese, as well as small amounts of copper, aluminum, and iron impurities. A holistic recycling process, besides the recovery of valuable metals, should also include the recovery of carbon due to its critical importance within the European economy [11,25–32].

The hydrometallurgical process route enables the targeted recovery of the valuable metals nickel and cobalt, as well as lithium and manganese from the black mass. Figure 2 shows the process routes that are currently employed for end-of-life batteries. For the wet chemical processing of the batteries, large quantities of chemicals are required for leaching and for the selective extraction steps, as well as for wastewater treatment. This is offset by lower energy requirements, due to the use of lower temperatures than in the pyrometallurgical route, as well as a higher recovery rate with greater end-product purity [33,34].

Due to the biogenic production methods of organic acids, they are considered potentially non-hazardous to the environment. By using organic acids as leaching agents, there is no secondary contamination, delayed corrosion, or increased occupational safety due to the reduced exposure to hazardous exhaust gases, and they are capable of selectively leaching metals. Organic carboxylic acids are biodegradable and the resulting waste from leaching is easy to handle; in addition, the acids can be processed and recirculated. By forming organo-metallic complexes, the metal ions can be dissolved and either selectively precipitated or extracted. Currently, these acids are more expensive than inorganic acids, due to their low commercialization in hydrometallurgy because of their increased pKa value, i.e., their weakly acidic character. Nevertheless, organic acids are able to achieve higher leaching rates than inorganic ones [33,35–40].

A broad spectrum of organic acids is currently being researched to achieve maximum leaching efficiencies when applied to different cathode materials or spent lithium-ion batteries. Citric acid, a three-protonic carboxylic acid, is one of the most widely studied forms [33,40–45].

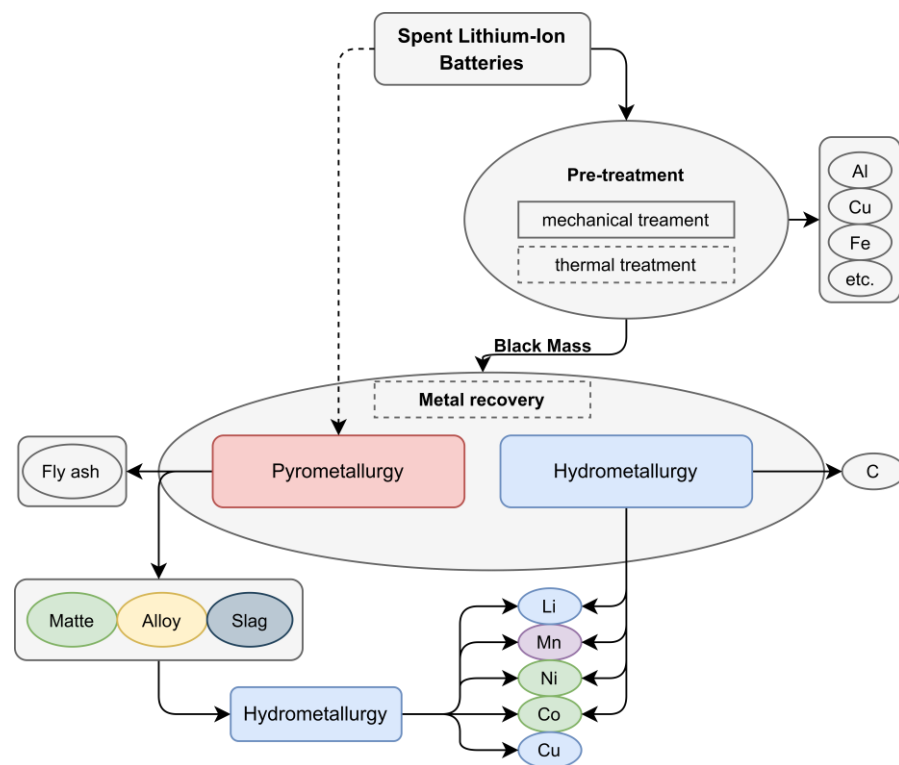


Figure 2. Schematic flow sheet of the processing paths of a spent lithium-ion battery.

In addition, oxalic, malic, tartaric, acetic, lactic, and formic acids are increasingly coming to the fore of scientific research [1,46–53]. In most studies, hydrogen peroxide is added as an oxidizing/reducing agent at different concentrations to achieve high recovery rates. The recovery rates prove H_2O_2 to be a necessary addition. However, self-decomposition poses a challenge in wet-chemical processes due to the exothermic reaction, which produces water and oxygen. In the context of non-toxic reaction products, H_2O_2 is considered to be a green reactant and can act as both an oxidizing and reducing agent. Therefore, the disproportionate level of peroxide in the presence of specific organic acids and metal ions is of great interest. A study by Gerold et al. [54] was able to show that the rate of decomposition due to catalytic processes depends on the organic acid and must be taken into account in test designs [54,55].

Biohydrometallurgy is a branch of hydrometallurgy that uses microorganisms to leach metals from ores, concentrates, and scrap metal and feeds the results into extractive metallurgy processes. This type of metal mobilization is attracting increasing attention because of its potential to recycle waste streams in an even more environmentally friendly way. The technique is cost-effective as it uses biologically produced solvents to treat the waste and requires very little industrial equipment. So far, ubiquitous chemolithotrophic, heterotrophic prokaryotes, bacteria, and fungi have been researched. The leaching step is aimed at dissolving the metal components from spent lithium-ion batteries and further processing them in a wet chemical process, as seen in conventional hydrometallurgy [56,57]. Do et al. [58] showed that a recovery rate of 89.9% Li, 90.4% Co, 91.8% Mn, and 85.5% Ni is possible by using *Acidithiobacillus ferrooxidans* (DSMZ 1926). *Aspergillus niger*, a well-known mold, can be stimulated to maximize the production of various organic acids. Balahoo Horeh et al. [59] succeeded in maximizing acid production along the citrate cycle and achieved leaching rates of 100% Li, 64% Co, 77% Mn, and 54% Ni by adapting the fungus to the suspension [58–60].

Previous biohydrometallurgical studies have demonstrated that gluconic acid can be produced either enzymatically or by the oxidative degradation of glucose. For example, Wang et al. [61] showed that the aldehyde group in glucose reduces the higher valent metals Ni^{3+} , Co^{3+} , and Mn^{4+} to the lower valent states of Ni^{2+} , Co^{2+} , and Mn^{2+} , as well as

changing the aldehyde group within glucose oxidizes to a carboxyl group; thus, glucose converts to gluconic acid, which, in turn, supports the leaching of metals. Therefore, more than 90% of the valuable metals can be dissolved by using malic acid and glucose. The oxidative degradation of glucose to gluconic acid and, further, to glycolic, glyceric, and formic acid is described by Sidiq et al. [62] in their study on the hydrometallurgical recycling process of NMC cathode materials, in which the authors use malic acid in combination with glucose as a reducing agent. The leaching step achieved an efficiency of 95%. Liang et al. [63] investigated the leaching efficiency of acetate acid when used with glucose as a reducing agent, with a leaching rate of more than 97% for the valuable metals. However, the oxidative degradation of glucose to gluconic acid has not been investigated further. The use of glucose as a reducing agent was also investigated by Choi et al. [43], Chen et al. [64], and Yao et al. [65], employing it with citric acid for spent lithium-ion battery materials. In the aforementioned studies, leaching rates of more than 92% were achieved for the individual valuable metals at the respective parameters investigated, whereas Chen et al. [64], as well as Yao et al. [65], described the oxidative degradation of glucose to gluconic acid and the associated improvement of the leaching process [43,61–65].

Gluconic acid, D-gluconic, dextransonic acid, or 2,3,4,5,6-pentahydroxyhexanoic acid is mainly produced via fermentation using *A. niger*, which utilizes glucose as a major carbohydrate source and converts it into gluconic acid via the enzymatic activity of glucose-1-oxidase. Therefore, production can be realized by using this enzymatic reaction. This acid can be found in humans and in other organisms. Gluconic acid is employed as a bulk chemical in food, animal feed, and the beverage, textile, pharmaceutical, and construction industries for its excellent chelating properties [66–70].

Several studies investigated biogenically produced gluconic acid and the leaching behavior of this acid for leaching rare earth elements, as well as base metals, from different sorts of batteries or from printed circuit boards. However, most studies are limited to studying the presence of gluconic acid in bioleaching processes using various bacteria and fungi [71–75].

In wet chemical processing, the biogenic components produce gluconic acid, as well as hydrolyzed glucono- δ -lactone dissociate in water (see Formula (1)) and lead to a decrease in pH [60].



The conjugate base of the dissociated organic acid subsequently acts as a chelating agent for the mono-, di- and trivalent cations (see Formula (2)) [60].



For this reason, gluconic acid was investigated for its possible utilization in the recycling processes for spent lithium-ion batteries. Roshanfar et al. [76] investigated lactonic and gluconic acid with regard to their leaching efficiency and showed that they are suitable for dissolving valuable metals such as lithium, as well as cobalt [76].

Fan et al. [77] investigated the leaching behavior of enzymatically prepared gluconic acid on NMC cathode materials. For this purpose, spent lithium-ion batteries were disassembled and pretreated in N-methyl-2-pyrrolidone to remove both the organic binder and the aluminum foil. Carbon and polyvinylidene difluoride were then removed by heating the material in a muffle furnace at 700 °C. Subsequent gluconic acid leaching with hydrogen peroxide yielded leaching rates of 96.27% for Li, as well as 96.45% for Mn, 95.49% for Co, and 96.53% for Ni [77].

2. Materials and Methods

Pyrolyzed NMC black mass was used for the study. The average mass composition was determined by a triplet of ICP-MS measurements (ICP-MS; Agilent 8800, Santa Clara, CA, USA) in order to determine the leaching efficiency of the valuable metals and the accompanying metals. The composition of the black mass is given in Table 1.

Table 1. Chemical composition of the NMC black mass.

Element	Li	Ni	Co	Mn	Cu	Al	Fe
wt %	3.4	22.2	6.2	7.3	5.9	4.4	0.5

2.1. Materials and Reagents

This study used D-(+)-Glucono-1,5-lactone (99%, Thermo Fisher, Kandel, Germany) to investigate the dissolution behavior of spent NMC black mass. The black mass used in this study originated from spent lithium-ion batteries that had been pyrolyzed to remove the organic components and the binder. The influence of hydrogen peroxide (30%, Carl Roth, Karlsruhe, Germany) as an oxidizing/reducing agent was also investigated. By varying the leaching parameters, such as acid and oxidant concentrations, temperature, the solid–liquid ratio, and the leaching time, a testing range with high leaching efficiency could be identified (see Table 2).

Table 2. Selected parameter limits for the study.

Parameter	Minimum Value	Maximum Value
C ₆ H ₁₀ O ₁₀ (mol/L)	0.5	1.5
H ₂ O ₂ (vol %)	0	2
Temperature (°C)	30	75
S/L ratio (g/L)	25	100
Leaching time (min)	30	240

2.2. Experimental

A double-walled flat-bottomed glass reactor was used as the reactor vessel. The temperature was controlled by means of a thermostat (Lauda, P 8C X, Lauda-Königshofen, Germany). Due to the crystalline nature of the acid, the acid was first dissolved in 200 mL of distilled water before the cathode material was added to the nitrogen-flooded vessel via funnels. N₂ was used to set a defined atmosphere so that a defined oxygen potential was provided in the experiment. The stirring speed was set at 400 rpm for all experiments to ensure the sufficient mixing of the liquid and solid to form a homogeneous suspension. The necessary amount of hydrogen peroxide was added to the mixture by means of dropping funnels. Figure 3 shows the experimental setup schematically. The start time of the leaching process was marked by the complete addition of the reagents required for the experiments; thus, this was either the addition of an oxidant or, in the case of experiments that did not require the addition of hydrogen peroxide, the completed addition of the black mass. After the leaching period was completed, the solids were separated by vacuum filtration. The solid residue was dried at 105 °C for at least 24 h.

2.3. Analytical Methods

To determine the leached amounts of lithium, nickel, manganese, and cobalt in the filtrate, a microwave plasma atomic emission spectrometer (4210 MP-AES, Agilent, Santa Clara, CA, USA) was used. The analysis of results was performed with the aid of the statistical program MODDE 12 (Sartorius AG, Göttingen, Germany). The software was used at the beginning of the experimental process to create a D-optimal experimental design with three center trials. To determine the influences of the individual target parameters (acid concentration, oxidant concentration, temperature, leaching duration, and S/L ratio), 32 individual tests were performed. Within this model, it was possible to consider the interactions of parameters. The qualitative investigation of the filter residues was performed using a scanning electron microscope (JEOL IT-300 LV, Tokyo, Japan) for energy dispersive measurement. The detector used was an EDS detector from Oxford Instruments (X-Max^N, 50 mm², Abingdon, UK). The parameters for the EDS measurements were chosen to be 15 kV, with a 10.2 mm working distance (WD).

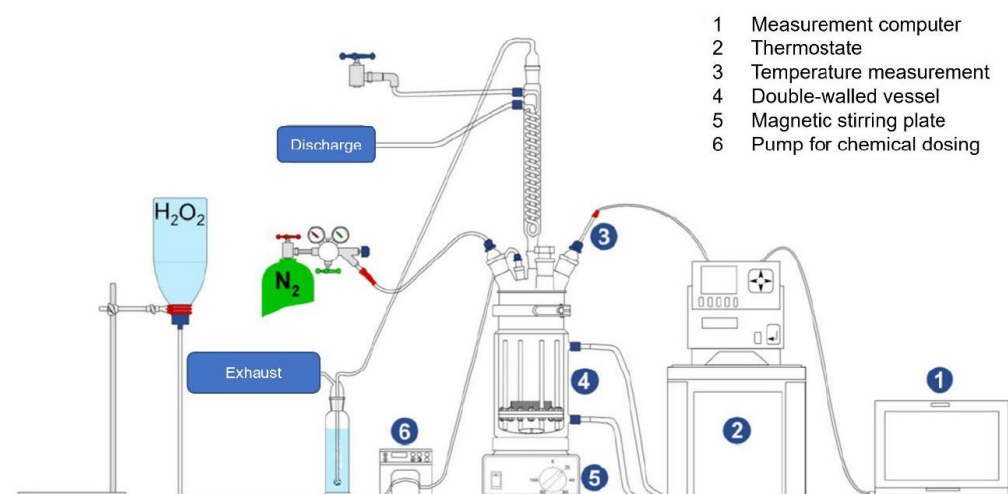


Figure 3. Schematic diagram of the experimental setup for the execution of the tests with NMC black mass (Reprinted from ref. [78]).

3. Results

In this section, first, contour plots, factor analyses, and optimization calculations were prepared to ensure a clear presentation of the results of the obtained concentrations. In the second part, selected residues from the filtration process were evaluated by applying SEM/EDS.

3.1. Leaching Behavior of Valuable Metals

The focus of the results is on the maximum feasible extraction of lithium, cobalt, manganese, and nickel from the black mass by varying the gluconic acid and hydrogen peroxide concentrations. The tested leaching parameters are given in Table 3. The data that were obtained form the basis for the evaluation in the statistics program and represent the real leaching behavior. The maximum contents obtained for lithium ($2.65 \text{ g}\cdot\text{L}^{-1}$), Co ($4.52 \text{ g}\cdot\text{L}^{-1}$), Ni ($10.89 \text{ g}\cdot\text{L}^{-1}$), Mn ($6.49 \text{ g}\cdot\text{L}^{-1}$), Fe ($0.13 \text{ g}\cdot\text{L}^{-1}$), Cu ($1.13 \text{ g}\cdot\text{L}^{-1}$), and Al ($2.45 \text{ g}\cdot\text{L}^{-1}$) are of particular interest with respect to the achievable leaching rates.

Figure 4 shows the statistical results as contour plots for the valuable metals, i.e., lithium, cobalt, nickel, and manganese, as a function of temperature and leaching time at a constant solid-to-liquid ratio of 25 g/L , an acid concentration of 1.5 in molarity, and varying oxidant concentrations. As the results show, significantly higher concentrations of nickel and cobalt can be found with higher oxidant additions (Figure 4c,f,i,l) than with no addition (Figure 4a,d,g,j) or minor additions (Figure 4b,e,h,k). The manganese content in the solution decreased slightly with increasing peroxide concentration, although the yield was almost complete with respect to the applied manganese concentration in the active material. Maximum lithium concentrations can be achieved with an average use of H₂O₂ (Figure 4b). With respect to the analysis of the black mass, however, the highest amounts of lithium can be dissolved with a higher level of hydrogen peroxide. As shown in the evaluation, the solubility behavior of the elements is strongly dependent on the leaching parameters. For example, the highest concentrations of lithium are obtained at a constant solid-to-liquid ratio of 25 g/L at moderate temperatures of about $55 \text{ }^\circ\text{C}$, with leaching times of 180 min and a medium quantity of hydrogen peroxide. In order to dissolve the manganese completely, a duration of 240 min, an acid concentration of 1 mol/L , and a temperature of $75 \text{ }^\circ\text{C}$ are required. Further small additions of H₂O₂ increased the manganese concentration in the solution. Parameter changes were not as pronounced compared to those for Li, Ni, and Co, which is why Mn can generally be found in significant amounts. Nickel and cobalt show very similar mobilization behavior, with Co dissolving almost completely at appropriate parameter settings. As the results show, the highest concentrations can be detected after longer leaching times of over 200 min, a H₂O₂

concentration of 2 vol %, and a temperature of 75 °C. In general, for the metals investigated, the concentration increased significantly with an increase in the amount of pyrolyzed black mass that was added. However, doubling the solid input did not double the dissolved amount. Accordingly, the highest leaching rates resulted in a low solid content in the suspension. The governing factors on the individual main metallic components in the black mass are presented in the parameter analysis discussed in Section 3.2.

Table 3. Statistical experimental design for an investigation of the leaching behavior of NMC black mass.

No.	Acid Concentration	Oxidant Concentration	Temperature	Solid/Liquid Ratio	Leaching Time
-	(mol·L ⁻¹)	(vol %)	(°C)	(g·L ⁻¹)	(min)
N1	0.5	2	30	25	30
N2	0.5	0	60	25	30
N3	1.5	2	60	25	30
N4	1	1	75	25	30
N5	1.5	1	30	50	30
N6	0.5	0	30	100	30
N7	1.5	2	30	100	30
N8	1.5	0	75	100	30
N9	0.5	2	75	100	30
N10	1.5	0	30	25	60
N11	1.5	0	75	25	60
N12	0.5	0	75	50	60
N13	1.5	2	75	50	60
N14	1	1	45	100	60
N15	1.5	0	60	100	60
N16	1	2	30	25	120
N17	1.5	2	45	100	120
N18	0.5	1	60	100	120
N19	0.5	0	30	25	240
N20	1.5	2	30	25	240
N21	1.5	0	75	25	240
N22	0.5	2	75	25	240
N23	0.5	2	45	50	240
N24	1	0	60	50	240
N25	1.5	0	30	100	240
N26	0.5	2	30	100	240
N27	0.5	0	75	100	240
N28	1.5	1	75	100	240
N29	1	2	75	100	240
N30	1	1	60	50	120
N31	1	1	60	50	120
N32	1	1	60	50	120

3.2. Parameter Study on the Leaching Behavior of Selected Elements

This section deals with the dissolution behavior of the valuable metals present in the black mass. It appears that due to thermodynamic differences and the implementation of the leaching process, different concentrations result in the dependence of the parameters. These are shown in detail for the individual elements, with otherwise medium settings. Medium settings are defined as an acid concentration of 1 mol/L, an oxidant addition of 1 vol %, a temperature of 60 °C, a leaching time of 120 min, and an S/L ratio of 50 g/L.

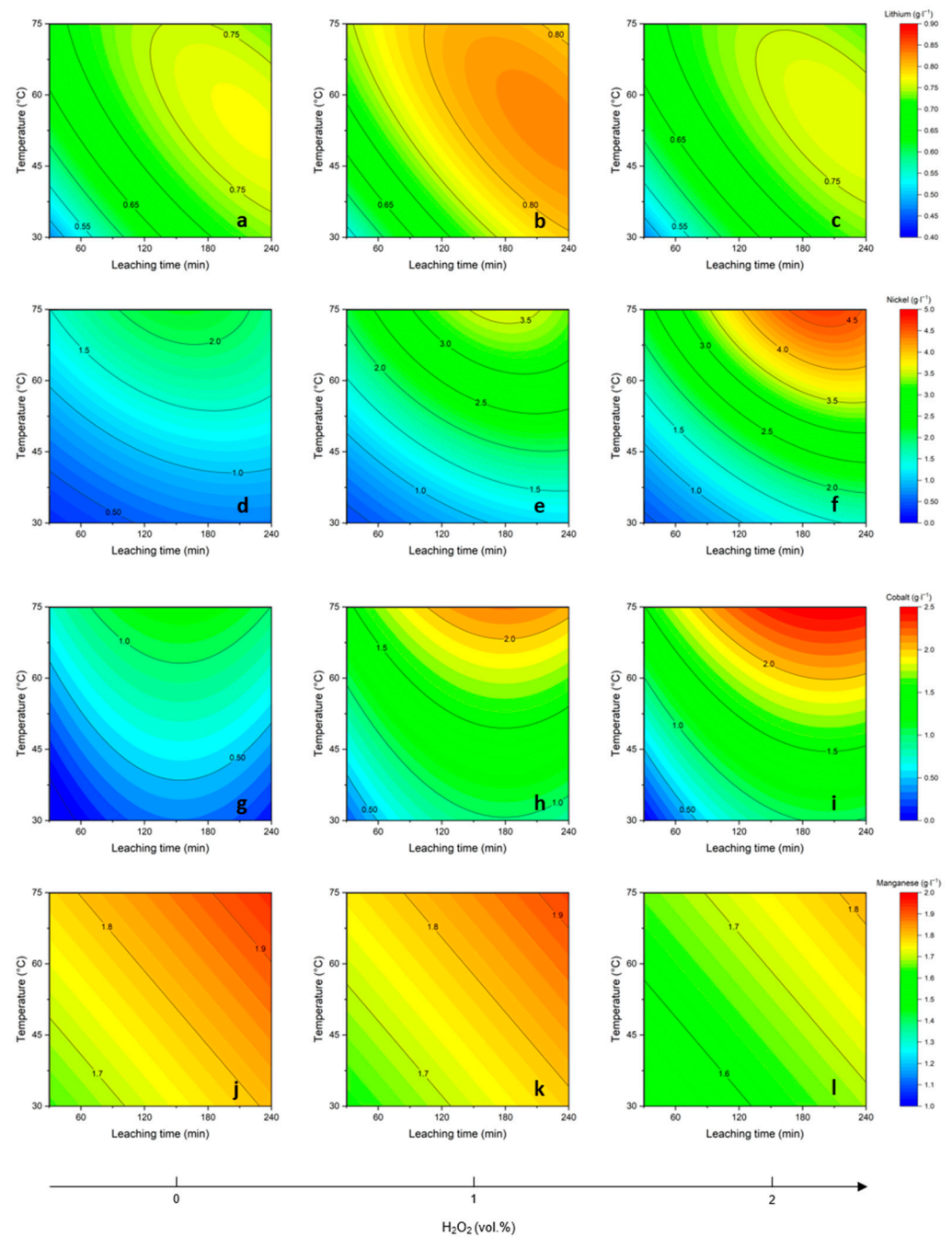


Figure 4. Contour plots obtained as a function of temperature versus leaching time for a 1.5 M solution with a solid-to-liquid ratio of 25 g/L for lithium at an addition of (a) 0 vol %, (b) 1 vol %, and (c) 2 vol % of H_2O_2 , for cobalt at an addition of (d) 0 vol % of H_2O_2 , (e) 1 vol % of H_2O_2 , and (f) 2 vol % of H_2O_2 , and for nickel at an addition of (g) 0 vol % of H_2O_2 , (h) 1 vol % of H_2O_2 , and (i) 2 vol % of H_2O_2 , as well as manganese at an addition of (j) 0 vol % of H_2O_2 , (k) 1 vol % of H_2O_2 , and (l) 2 vol % of H_2O_2 .

3.2.1. Lithium

Lithium was detected in the respective filtrates at concentrations ranging from 0.58 to 2.65 g/L, depending on the set parameters. The amount of dissolved Li did not increase proportionally with the amount of black mass used. Up to a solid-to-liquid ratio of 50 g/L, the metal content increased by a factor of 1.6 and subsequently reduced to 1.4 at an S/L ratio of 100 g/L, using the medium settings of the other parameters. Figure 5 shows the described behavior using a 95% confidence interval for the achievable lithium concentration

in solution as a function of the solid-to-liquid ratio. Accordingly, the highest leaching rates resulted from a low-level addition of black mass to the leach. Additionally, the highest metal contents of lithium required 0.9 mol/L of acid and 1 vol % of oxidizing agent. The data show that an increase in temperature with intermediate settings of the other parameters increased the achievable lithium concentration by about 44%, whereas maximizing the leaching time led to an increase of approximately 20%.

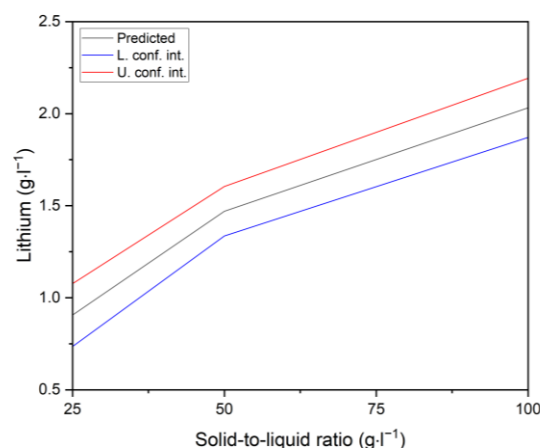


Figure 5. Representation of achievable lithium concentrations in solution at the mean parameter settings as a function of the solid-to-liquid ratio, with a 95% confidence interval.

3.2.2. Cobalt

The dissolved amount of cobalt was differentiated to a greater extent than that of lithium and was strongly dependent on the leaching parameters that were set. The measured concentrations ranged from 0.4 to 4.52 g/L in the solution. The greatest influence on the leaching behavior was exerted by the temperature, the choice of leaching time, and the amount of hydrogen peroxide added at medium settings. The influence of acid concentration and the solid-to-liquid ratio was present but was not as pronounced. For example, leaching efficiency could be increased by 66% by increasing the leaching time from 30 to 120 min. A further increase did not lead to a significant improvement in cobalt yield. On the one hand, even the achievable metal content in the solution decreased with a further increase of the oxidant concentration of about 1% by volume. On the other hand, leaching at 75 °C led to an enlargement of about 80% in the achievable concentration of Co compared to leaching at 30 °C (see Figure 6). A similar behavior is shown with an increase in acid concentration, but it is not seen to the same extent as that already mentioned under the influence of temperature.

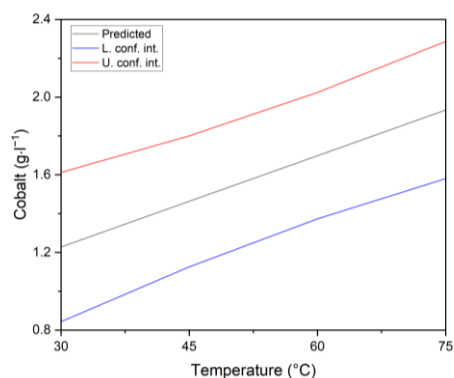


Figure 6. Representation of achievable cobalt concentrations in solution at the mean parameter settings, shown as a function of temperature at a 95% confidence interval.

3.2.3. Nickel

The dissolution properties of nickel are similar to those of cobalt, due to the chemical similarity of these two elements, which is partly due to their positions in the periodic table. The oxidant concentration exerts the greatest influence on the leaching efficiency. For example, the addition of 2 vol % of hydrogen peroxide doubles the achievable nickel concentration in solution, compared to experiments without the addition of an oxidizing/reducing agent. At medium settings (1 M $C_6H_{12}O_7$ and 1 vol % of H_2O_2), the leaching rate can be significantly increased, up to 60 °C; the temperature influence then decreases slightly afterward, up to 75 °C. With the addition of 1.5 mol/L of gluconic acid, as well as 2 vol % of hydrogen peroxide, the influence of temperature was more pronounced, resulting in the highest nickel contents seen at low solid contents. A high solid-to-liquid ratio of above 50 g/L significantly reduced the nickel yield.

3.2.4. Manganese

Compared to the other valuable metals, manganese can be readily transferred into a solution from the black mass. The maximum achievable quantity depends, essentially, on the acid concentration. The results show that a gluconic acid concentration of 1 mol/L is advantageous and exhibits the highest efficiencies for Mn at 75 °C. Figure 7 shows the effect of acid concentrations on the leaching efficiency of manganese at a 95% confidence interval. Too low, as well as too high, an addition of glucono- δ -lactone leads to low yields of the metal being leached from the black mass. The addition of more than 1 vol % of H_2O_2 has a minor negative effect on the concentration of the metal in the solution. Otherwise, the results show that a longer residence time increases the maximum amount of manganese in the solution that can be achieved.

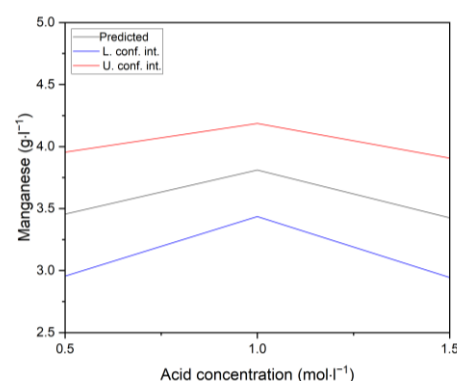


Figure 7. Representation of the achievable manganese concentration in solution at the mean parameter settings, shown as a function of acid concentration at a 95% confidence interval.

3.2.5. Accompanying Elements

The analysis of the samples for the main impurities of copper, aluminum, and iron shows different solution behaviors, depending on the set parameters. The selection of these elements was based on the fact that these metals represent the main impurities and negatively influence the further processing steps and reduce the product quality.

- Copper

Maximum copper concentrations were found at high acid as well as oxidant concentrations, at low temperatures, with a low solid-to-liquid ratio, and after short leaching times. High S/L ratios demonstrated lower Cu contents as a function of leaching duration. Furthermore, the content reduced significantly with the increasing residence time of the solids in the solution. High temperatures also resulted in negligible contents of copper in the solution, regardless of acid and oxidant concentrations. The influence on Cu concentration at medium parameter settings is shown in Figure 8.

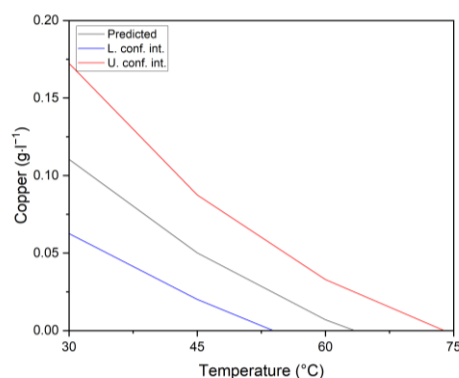


Figure 8. Representation of the achievable copper concentration in solution at mean parameter settings as a function of temperature, at a 95% confidence interval.

- Iron

Iron showed low solubility, regardless of the selected experimental settings, even at higher solid-to-liquid ratios. Only small amounts of iron, approximately 0.12 g/L, could be detected, although 0.5 wt % of iron was detectable in the black mass.

- Aluminum

The concentration of aluminum, which could be obtained in the individual tests, varied within a range from 0.54 to 2.52 g/L. The maximum achievable concentration depended mainly on the acid concentration, the leaching temperature, and the solid-to-liquid ratio. The leaching time had no significant influence, while the addition of an oxidizing/reducing agent only slightly reduced the achievable content. The data show that the aluminum concentration is proportional to the amount of black mass used. The influence of temperature is crucial since the highest amounts of metal, which could be found in the solution, were at an average temperature control of 75 °C. Figure 9 plots this behavior.

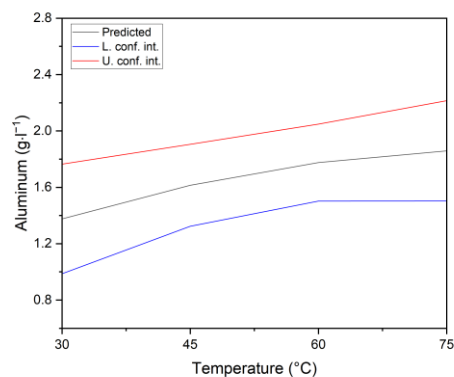


Figure 9. Representation of the achievable aluminum concentration in the solution at mean parameter settings, as a function of temperature at a 95% confidence interval.

3.3. Filter Residue Analysis

The solid residues recorded after filtration were examined via scanning electron microscopy. Conclusions were then drawn on the leaching behavior of the individual elements and phases using EDS, according to BSE uptake. The filter cakes from tests N3, N13, and N21 were investigated since those tests were closest to the optimum leaching conditions for achieving high leaching rates for the valuable metals lithium, nickel, cobalt, and manganese, and are discussed in the following section on the basis of the leaching parameters.

3.3.1. Filter Residue from N3

The powder sample from N3 was selected on the basis of the leaching parameters, which were essentially characterized by a high temperature (60 °C) and a high acid (1.5 M), as well as the peroxide concentration (2 vol %). In addition, this test was characterized by a leaching time of 30 min and a low solid-to-liquid ratio of 25 g/L. The BSE image shows lighter as well as darker particles at three different locations on the SEM stamp, which were analyzed via triplets on the EDS spectra. The analysis shows that the black grains consisted of pure carbon. Bright particles of light grayish and bright white can be identified. The chemical analysis indicated aluminum, as well as carbon and oxygen, as the main component in a range of between 39 and 63 wt %. In addition, nickel and cobalt could be detected in the spectrum at a very low range. Figure 10 shows an EDS mapping procedure for the determined elements in a selected area of the powder sample. A 1000× magnification was selected for the evaluation. Due to the roughness of the dissolved oxidic particles, aluminum and copper particles were found on the surface, in addition to nickel, cobalt, and manganese. Aluminum occurred in areas of high oxygen density, which is why an oxidic phase can be assumed.

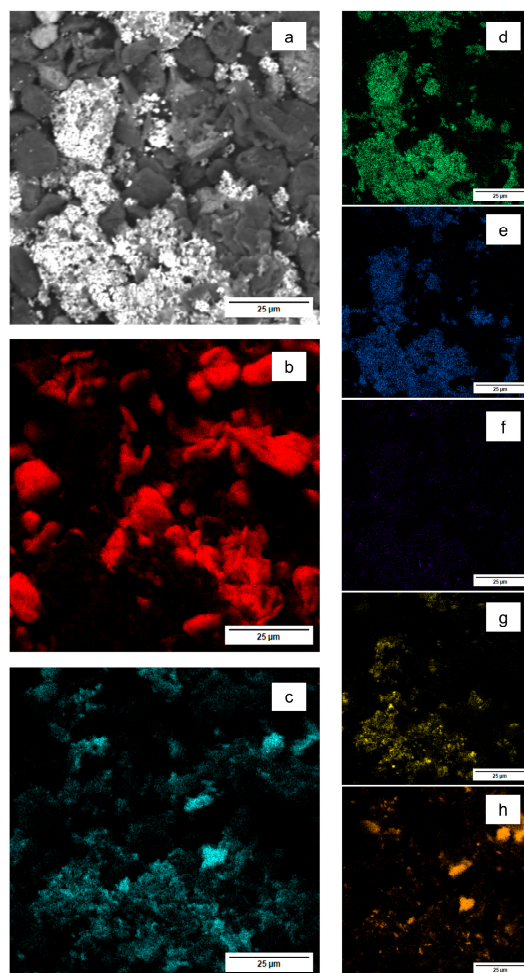


Figure 10. EDS mapping of sample N3, showing (a) the uptake range and element spectra for (b) carbon, (c) oxygen, (d) nickel, (e) cobalt, (f) manganese, (g) copper, and (h) aluminum at 1000× magnification.

3.3.2. Filter Residue from N13

As with sample N3, the BSE image of experiment N13 shows very light, grayish, and dark particles. The leaching parameters for N13 were an acid concentration of 1.5 M gluconic acid, an addition of 2 vol % of hydrogen peroxide, a leaching temperature of 75 °C,

a solid-to-liquid ratio of 50 g/L, and a leaching time of 60 min. For the evaluation, three different areas of the powder sample were used for an elemental analysis of the individual particles, and triplets of spectra were made. According to this analysis, the compound of the very bright grains comprised an oxidic compound of nickel and cobalt. Similar to N3, the grayish particles were composed of about 42 wt % of aluminum and oxide. Manganese could only be detected in three spectra, in combination with nickel, cobalt, and oxide. In the EDS mapping, shown in Figure 11, a region without the detection of manganese is shown. The elemental analysis indicates the presence of carbon as single particles and nickel associated with cobalt, both with and without oxygen, as well as aluminum and copper particles in the powder, shown at 1000 \times magnification.

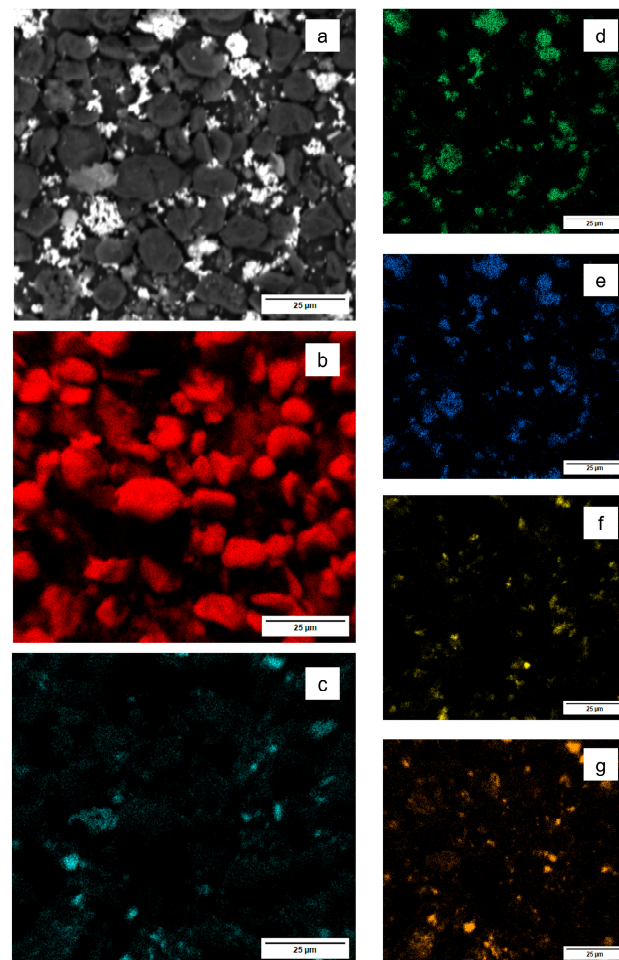


Figure 11. EDS mapping of sample N13, showing the (a) uptake range and element spectra for (b) carbon, (c) oxygen, (d) nickel, (e) cobalt, (f) copper, and (g) aluminum at 1000 \times magnification.

3.3.3. N21

N21 represents a range with high leaching efficiency, in terms of leaching parameters, but without the use of hydrogen peroxide, which is why this test was chosen for a detailed evaluation. Leaching was carried out with the addition of 1.5 mol/L glucono- δ -lactone at a temperature of 75 $^{\circ}$ C, a solid-to-liquid ratio of 25 g/L, and a leaching time of 240 min. Analysis of the filter residue, shown in the BSE image, demonstrates both very light and dark particles on the sample stamp. Triplets of the spectra were made for the different brightness particles, at three different locations for each, to determine their composition. In the elemental analysis, the dark grains consisted of almost pure carbon. The light particles showed a composition of oxygen, nickel, and cobalt, with Ni to Co in a molar ratio of 3:1. In addition, copper and small amounts of aluminum could be detected. The element distribution of the EDS mapping is shown in Figure 12, demonstrating a clear

elemental distribution. The dark particles consisted of carbon, while the bright areas of the components consisted of oxygen, nickel, cobalt, manganese, copper, and aluminum. The areas with oxygen overlapped the areas of Ni, Co, Al, and partly Mn, overlapping only weakly those areas with copper. The EDS mapping suggests that aluminum was present as an oxidic phase.

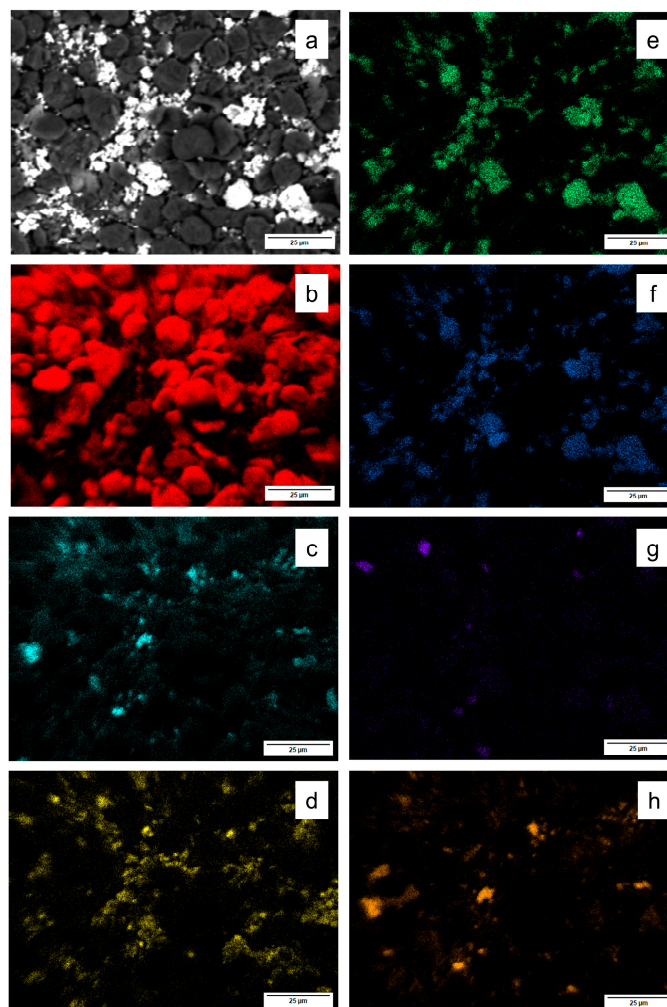


Figure 12. EDS mapping of sample N21, showing the (a) uptake range and element spectra for (b) carbon, (c) oxygen, (d) copper, (e) nickel, (f) cobalt, (g) manganese, and (h) aluminum, at 1000× magnification.

4. Discussion

In order to achieve high leaching efficiency from NMC black mass, a comprehensive knowledge of the influencing parameters and their interactions within the leaching process is essential. The results suggest that depending on the degree of contamination, especially with aluminum, factor analysis is necessary on both the elemental and material levels. Through a broad analysis of the results, acid concentration, oxidant addition, temperature, solid-to-liquid ratio, and leaching time can be identified as the main parameters influencing leaching.

For a complete evaluation, an optimization calculation was performed using the statistical program MODDE 12.1, with the objective of achieving the highest possible leaching efficiency for the valuable metals, lithium, cobalt, nickel, and manganese, which are present in the black mass. Gluconic acid is already used in various industries (food, pharmaceuticals, textiles, etc.) and is an organic acid with good complexing properties and a pKa value of 3.86. Gluconic acid is industrially produced, mainly biologically or

enzymatically, and is generally considered to be environmentally friendly. Accordingly, high leaching rates for the valuable metals, lithium, nickel, cobalt, and manganese require an acid concentration of 1.15 M of glucono- δ -lactone, 1.6 vol % of hydrogen peroxide, a leaching time of 192 min, a temperature of 75 °C, and a solid-to-liquid ratio of 25 g/L, where the solid addition is fixed. A long leaching time, in combination with a high set temperature, has a positive effect on the dissolved amounts of copper, which would otherwise negatively oppose further processing.

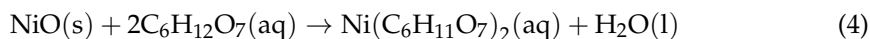
As can be seen in Figure 4 in Section 3.1, the amount of hydrogen peroxide provided in the experiment turned out to be an essential parameter. The addition of the total amount of oxidant/reductant agent at the beginning of the individual tests proved to be disadvantageous. Hydrogen peroxide decomposes quickly, particularly when the heavy metals Cu, Fe, Mn, Ni, and Co are present, which have a catalytic effect on the decomposition reaction.

Depending on the metallic phase that is present after pyrolysis, the addition of hydrogen peroxide as an oxidizing/reductant agent is necessary to induce a suitable oxidation state in the components. According to the literature, Co_3O_4 , NiO, Mn_3O_4 , Li_2CO_3 , Li_2O , CoO, MnO, MnO_2 , LiNiO_2 , LiAlO_2 , and Al_2O_3 , as well as metallic Ni, Co, Mn, Cu, and Al can be found in the black mass, depending on the selected temperature settings and the holding periods used in the process [25,30,79].

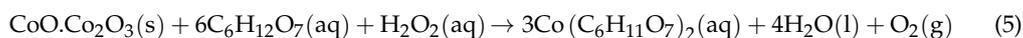
The metallic as well as oxidic components of the pyrolyzed powder can be dissolved by the oxidizing/reducing agent via acid consumption, according to Equation (3), resulting in a need for hydrogen peroxide, whereas a soluble stable oxidation state of the valuable metal can be formed.



The divalent metal oxides are soluble, due to their oxidation state, and form the corresponding metal complexes with the acid presented. As an example, for NiO, MnO, and CoO, the reaction is given by Equation (4).



The conversion of trivalent metal ions from the oxidic compounds into a soluble form occurs via the reduction of the oxide with hydrogen peroxide and the subsequent dissolution of the divalent metal oxide with gluconic acid, resulting in the formation of an organometallic complex. This requires a simultaneous attack by both the acid and the hydrogen peroxide (Equation (5)).



Some transition compounds exist that require electron transfer for dissolution, in addition to acidic conditions. The results of the residue analysis in Section 3.3 show nickel compounds, some of which are associated with cobalt, manganese, aluminum, and oxygen. To dissolve this valuable fraction, the presence of hydrogen peroxide is crucial; however, this rapidly degrades due to the temperatures and the metals involved.

The highest leaching efficiencies can be achieved at low S/L ratios. Although the concentration of metal ions in solution increases with an increase in the volume of solids, the amount does not double with a doubling of the feedstock. Acid concentrations that are too low result in a significant shift in the pH toward weakly alkaline conditions with a high solid-to-liquid ratio of basic input material and also lead to reduced leaching efficiency, due to the stability ranges of the valuable metals. The optimization of oxidant/reductant addition will be investigated in future works and will provide information on the maximum achievable partition coefficients between the solid and solution. The values seen in the ICP-MS analysis of the black mass, used in combination with an optimization calculation, show very high leaching efficiencies of almost 99% at a solid-to-liquid ratio of 25 g/L. The

Ni-containing residues, as seen in Section 3.3, reduce the nickel yield to 80%, which is why the phase determination of the residue will be considered in future works.

5. Conclusions

Lithium-ion batteries have emerged as crucial technology in our modern world, by enabling the creation of portable electronics, electric vehicles, and decentralized energy storage. LIBs offer high energy density along with good scalability. The sharp increase in electric vehicle sales, which is the result of government incentives, such as implemented policies, financial incentives, such as reduced taxes, or prohibition of the sale of non-CO₂-neutral powered passenger vehicles from 2035 onward has led to an increased demand for certain raw materials, especially critical raw materials such as copper, nickel, cobalt, manganese, lithium, and graphite. The possibility of achieving strategic independence from foreign markets highlights the need to recycle spent LIBs, while at the same time, energy production and the associated additional CO₂ emissions can be reduced.

The hydrometallurgical recycling of materials, in addition to the above-mentioned advantages, offers the possibility of recovering valuable metals at high purity and in high proportions, with a reduced energy requirement. Due to their high availability, low price, and good properties, the wet chemical processes, both primary and secondary, used in industry work with strong inorganic acids. These are environmentally intolerable and, in addition to increased labor law safety standards (regarding emissions and toxic effects), necessitate downstream reprocessing and a suitable landfill for residual materials.

Efforts are being made within the research community to make the hydrometallurgical process more sustainable, which is why organic acids are the focus of much research attention. Compared to mineral acids, organic acids are more expensive and of weak character, but they can form soluble metal complexes. Their advantage lies in their high environmental compatibility as these acids are mostly produced biologically and are biodegradable, with a significantly lower CO₂ footprint.

Gluconic acid can be produced either biologically, via *Aspergillus niger* or *Gluconobacter*, or enzymatically. To achieve a sustainable recycling process, gluconic acid is a suitable candidate due to its favorable properties.

The study shows that gluconic acid exhibits the highest leaching rates for the valuable metals Li, Co, Ni, and Mn at low solid-to-liquid ratios. An optimization calculation was carried out using the data that were obtained, which shows that high leaching rates can be achieved, even at low concentrations of acid (1.2 M) and hydrogen peroxide (1.6 vol %), at a temperature of 75 °C and a solid-to-liquid ratio of 25 g/L, within 192 min. Accordingly, the valuable metals Li, Co, and Mn can be dissolved almost completely, along with Ni at about 81%.

Future works will deal with the optimization of oxidant addition, as well as the reduction in H₂O₂ for process control, and will examine how these changes affect the remaining parameters. Gluconic acid is also to be applied to black matter from other LIBs' black masses. Further investigations under these optimized parameters will aim to identify the valence states of the metal ions in the complex and also in solution, as well as to determine the phases in the solid residue. They will also investigate the reusability of the acid, as already suggested in the literature, in order to clarify a possible new and economic recycling route. The overarching objective is to work with enzymatically and biologically produced acids, in order to open up a possible biohydrometallurgical route that combines the advantages of low cost with low energy input, while simultaneously ensuring the universality of the application material.

Author Contributions: Conceptualization, R.L.; methodology, R.L. and E.G.; software, R.L.; validation, R.L., E.G. and H.A.; formal analysis, R.L.; investigation, R.L.; resources, E.G.; data curation, R.L.; writing—original draft preparation, R.L. and E.G.; writing—review and editing, R.L., E.G. and H.A.; visualization, R.L.; supervision, E.G. and H.A.; project administration, E.G.; funding acquisition, H.A. All authors have read and agreed to the published version of the manuscript.

Funding: This research received no external funding.

Data Availability Statement: The data presented in this study are available on request from the corresponding author. The data are not publicly available due to privacy restrictions.

Conflicts of Interest: The authors declare no conflict of interest.

References

1. Meshram, P.; Mishra, A.; Sahu, R. Environmental impact of spent lithium ion batteries and green recycling perspectives by organic acids—A review. *Chemosphere* **2020**, *242*, 125291. [CrossRef]
2. Kresse, C.; Bastian, D.; Bookhagen, B. *Lithium-Ionen-Batterierecycling in Deutschland und Europa*; Bundesanstalt für Geowissenschaften und Rohstoffe: Hannover, Germany, 2022.
3. Zechmeister, A.; Anderl, M.; Bartel, A.; Frei, E.; Gugele, B.; Gössl, M.; Mayer, S.; Heinfellner, H.; Heller, C.; Heuberger, A.; et al. *Klimaschutzbericht 2022*; Report; Umweltbundesamt: Wien, Austria, 2022.
4. Statista: Annual Greenhouse Gas Emissions in the European Union (EU-27) from 1990 to 2021, by Sector. Available online: <https://www.statista.com/statistics/1171183/ghg-emissions-sector-european-union-eu/> (accessed on 6 June 2023).
5. IEA. *Global Electric Vehicle Outlook 2022*; IEA: Paris, France, 2022.
6. Presse—Und Informationsamt der Bundesregierung: EU-Umweltrat: Nur Noch CO₂-Frei Fahren. Available online: <https://www.bundesregierung.de/breg-de/schwerpunkte/europa/verbrennermotoren-2058450> (accessed on 29 March 2022).
7. Vertretung in Deutschland: EU-Staaten Stimmen—Endgültig—Für Emissionsfreie Autos ab 2035. Available online: https://germany.representation.ec.europa.eu/news/eu-staaten-stimmen-endgultig-fur-emissionsfreie-autos-ab-2035-2023-03-28_de (accessed on 3 April 2023).
8. Europäische Kommission. *Der Europäische Grüne Deal—Mitteilung der Kommission an das Europäische Parlament, den Europäischen Rat, den Rat, den Europäischen Wirtschafts- und Sozialausschuss und den Ausschuss der Regionen—Der Europäische Grüne Deal*; Europäische Kommission: Brussels, Belgium, 2019.
9. Europäische Kommission. *Die Europäische Batterie-Allianz Macht Fortschritte: Gründung einer Europäischen Batterieakademie zur Verbesserung der Fähigkeiten für ein Rasch Wachsendes Batterieökosystem in Europa*; Europäische Kommission: Brussels, Belgium, 2022.
10. Europäische Kommission. *Verordnung des Europäischen Parlaments über Batterien und Altbatterien, zur Aufhebung der Richtlinie 2006/66/EG und zur Änderung der Verordnung (EU) 2019/1020*; Europäische Kommission: Brussels, Belgium, 2020.
11. European Commission. *Critical Raw Materials: Ensuring Secure and Sustainable Supply Chains for EU's Green and Digital Future*; European Commission: Brussels, Belgium, 2023.
12. *2023/0081 (COD)*; Verordnung des Europäischen Parlaments und des Rates zur Schaffung eines Rahmens für Maßnahmen zur Stärkung des Europäischen Ökosystems der Fertigung von Netto-Null-Technologieprodukten (Netto-Null-Industrie-Verordnung). European Commission: Brussels, Belgium, 2023.
13. Blengini, G.A.; Latunussa, C.E.L.; Eynard, U.; de Matos, C.T.; Wittmer, D.; Georgitzikis, K.; Pavel, C.; Carrara, S.; Mancini, L.; Unguru, M.; et al. *Study on the EU's List of Critical Raw Materials*; Publications Office of the European Union: Luxembourg, 2020.
14. Chen, M.; Ma, X.; Chen, B.; Arsenaull, R.; Karlson, P.; Simon, N.; Wang, Y. Recycling End-of-Life Electric Vehicle Lithium-Ion Batteries. *Joule* **2019**, *3*, 2622–2646. [CrossRef]
15. Brückner, L.; Frank, J.; Elwert, T. Industrial Recycling of Lithium-Ion Batteries—A Critical Review of Metallurgical Process Routes. *Metals* **2020**, *10*, 1107. [CrossRef]
16. Bernhart, W. Recycling von Lithium-Ionen-Batterien im Kontext von Technologie- und Preisentwicklungen. *ATZelektronik* **2019**, *14*, 38–43. [CrossRef]
17. Statista. Lithiumcarbonat: Preisentwicklung in den Jahren 2012 bis 2022. Available online: <https://de.statista.com/statistik/daten/studie/1323981/umfrage/preisentwicklung-fuer-lithiumcarbonat/?locale=de> (accessed on 3 April 2023).
18. Statista. Entwicklung des Aluminiumpreises Weltweit in den Jahren 1960 bis 2022. Available online: <https://de.statista.com/statistik/daten/studie/432518/umfrage/aluminiumpreis-weltweit/?locale=de> (accessed on 3 April 2023).
19. Statista. Durchschnittlicher Preis für Mangan Weltweit in den Jahren 2018 bis 2022. Available online: <https://de.statista.com/statistik/daten/studie/1361220/umfrage/durchschnittlicher-preis-fuer-graphit-weltweit/?locale=de> (accessed on 3 April 2023).
20. Statista. Durchschnittlicher Preis für Kupfer Weltweit in den Jahren 1960 bis 2022. Available online: <https://de.statista.com/statistik/daten/studie/432911/umfrage/durchschnittlicher-preis-fuer-kupfer-weltweit/?locale=de> (accessed on 3 April 2023).
21. Statista. Durchschnittlicher Preis für Kobalt Weltweit in den Jahren 2018 bis 2022. Available online: <https://de.statista.com/statistik/daten/studie/1366505/umfrage/durchschnittlicher-preis-fuer-indium-weltweit/?locale=de> (accessed on 3 April 2023).
22. Statista. Durchschnittlicher Nickelpreis Weltweit in den Jahren 1960 bis 2022. Available online: <https://de.statista.com/statistik/daten/studie/260594/umfrage/durchschnittlicher-nickelpreis/?locale=de> (accessed on 3 April 2023).
23. Windisch-Kern, S.; Gerold, E.; Nigl, T.; Jandric, A.; Altendorfer, M.; Rutrecht, B.; Scherhauser, S.; Raupenstrauch, H.; Pomberger, R.; Antrekowitsch, H.; et al. Recycling chains for lithium-ion batteries: A critical examination of current challenges, opportunities and process dependencies. *Waste Manag.* **2022**, *138*, 125–139. [CrossRef]

24. Jin, S.; Mu, D.; Lu, Z.; Li, R.; Liu, Z.; Wang, Y.; Tian, S.; Dai, C. A comprehensive review on the recycling of spent lithium-ion batteries: Urgent status and technology advances. *J. Clean. Prod.* **2022**, *340*, 130535. [[CrossRef](#)]
25. Li, J.; Lai, Y.; Zhu, X.; Liao, Q.; Xia, A.; Huang, Y.; Zhu, X. Pyrolysis kinetics and reaction mechanism of the electrode materials during the spent LiCoO₂ batteries recovery process. *J. Hazard. Mater.* **2020**, *398*, 122955. [[CrossRef](#)] [[PubMed](#)]
26. Ordoñez, J.; Gago, E.J.; Girard, A. Processes and technologies for the recycling and recovery of spent lithium-ion batteries. *Renew. Sustain. Energy Rev.* **2016**, *60*, 195–205. [[CrossRef](#)]
27. Raj, T.; Chandrasekhar, K.; Kumar, A.N.; Sharma, P.; Pandey, A.; Jang, M.; Jeon, B.-H.; Kim, S.H. Recycling of cathode material from spent lithium-ion batteries: Challenges and future perspectives. *J. Hazard. Mater.* **2022**, *429*, 128312. [[CrossRef](#)] [[PubMed](#)]
28. Shaw-Stewart, J.; Alvarez-Reguera, A.; Greszta, A.; Marco, J.; Masood, M.; Sommerville, R.; Kendrick, E. Aqueous solution discharge of cylindrical lithium-ion cells. *Sustain. Mater. Technol.* **2019**, *22*, e00110. [[CrossRef](#)]
29. Yang, Y.; Huang, G.; Xu, S.; He, Y.; Liu, X. Thermal treatment process for the recovery of valuable metals from spent lithium-ion batteries. *Hydrometallurgy* **2016**, *165*, 390–396. [[CrossRef](#)]
30. Lombardo, G.; Ebin, B.; Steenari, B.M.; Alemrajabi, M.; Karlsson, I.; Petranikova, M. Comparison of the effects of incineration, vacuum pyrolysis and dynamic pyrolysis on the composition of NMC-lithium battery cathode-material production scraps and separation of the current collector. *Resour. Conserv. Recycl.* **2021**, *164*, 105142. [[CrossRef](#)]
31. Nigl, T.; Nigl, T.; Rutrecht, B.; Altendorfer, M.; Scherhauser, S.; Meyer, I.; Sommer, M.; Beigl, P. Lithium-Ionen-Batterien—Kreislaufwirtschaftliche Herausforderungen am Ende des Lebenszyklus und im Recycling. *BHM Berg-Hüttenmännische Mon.* **2021**, *166*, 144–149. [[CrossRef](#)]
32. Doose, S.; Mayer, J.K.; Michalowski, P.; Kwade, A. Challenges in Ecofriendly Battery Recycling and Closed Material Cycles: A Perspective on Future Lithium Battery Generations. *Metals* **2021**, *11*, 291. [[CrossRef](#)]
33. Gerold, E.; Schinnerl, C.; Antrekowitsch, H. Critical Evaluation of the Potential of Organic Acids for the Environmentally Friendly Recycling of Spent Lithium-Ion Batteries. *Recycling* **2022**, *7*, 4. [[CrossRef](#)]
34. Gerold, E.; Luidold, S.; Antrekowitsch, H. Separation and Efficient Recovery of Lithium from Spent Lithium-Ion Batteries. *Metals* **2021**, *11*, 1091. [[CrossRef](#)]
35. Golmohammadzadeh, R.; Faraji, F.; Rashchi, F. Recovery of lithium and cobalt from spent lithium ion batteries (LIBs) using organic acids as leaching reagents: A review. *Resour. Conserv. Recycl.* **2018**, *136*, 418–435. [[CrossRef](#)]
36. Mohanty, A.; Devi, N. A Review on Green Method of Extraction and Recovery of Energy Critical Element Cobalt from Spent Lithium-Ion Batteries (LIBs). *Miner. Process. Extr. Metall. Rev.* **2023**, *44*, 52–63. [[CrossRef](#)]
37. Punt, T.; Akdogan, G.; Bradshaw, S.; van Wyk, P. Development of a novel solvent extraction process using citric acid for lithium-ion battery recycling. *Miner. Eng.* **2021**, *173*, 107204. [[CrossRef](#)]
38. Nayaka, G.P.; Zhang, Y.; Dong, P.; Wang, D.; Pai, K.V.; Manjanna, J.; Santhosh, G.; Duan, J.; Zhou, Z.; Xiao, J. Effective and environmentally friendly recycling process designed for LiCoO₂ cathode powders of spent Li-ion batteries using mixture of mild organic acids. *Waste Manag.* **2018**, *78*, 51–57. [[CrossRef](#)]
39. Li, L.; Bian, Y.; Zhang, X.; Xue, Q.; Fan, E.; Wu, F.; Chen, R. Economical recycling process for spent lithium-ion batteries and macro- and micro-scale mechanistic study. *J. Power Sources* **2018**, *377*, 70–79. [[CrossRef](#)]
40. Zheng, Q.; Watanabe, M.; Iwatate, Y.; Alzuma, D.; Shibazaki, K.; Hiraga, Y.; Kishita, A.; Nakayasu, Y. Hydrothermal leaching of ternary and binary lithium-ion battery cathode materials with citric acid and the kinetic study. *J. Supercrit. Fluids* **2020**, *165*, 104990. [[CrossRef](#)]
41. Nurqomariah, A.; Fajaryanto, R. Leaching and kinetics process of cobalt from used lithium ion batteries with organic citric acid. *E3S Web Conf.* **2018**, *67*, 3036.
42. Musariri, B.; Akdogan, G.; Dorfling, C.; Bradshaw, S. Evaluating organic acids as alternative leaching reagents for metal recovery from lithium ion batteries. *Miner. Eng.* **2019**, *137*, 108–117. [[CrossRef](#)]
43. Choi, J.-W.; Cho, C.-W.; Yun, Y.-S. Organic acid-based linear free energy relationship models for green leaching of strategic metals from spent lithium-ion batteries and improvement of leaching performance. *J. Hazard. Mater.* **2022**, *423*, 127214. [[CrossRef](#)]
44. Li, L.; Bian, Y.; Zhang, X.; Guan, Y.; Fan, E.; Wu, F.; Chen, R. Process for recycling mixed-cathode materials from spent lithium-ion batteries and kinetics of leaching. *Waste Manag.* **2018**, *71*, 362–371. [[CrossRef](#)] [[PubMed](#)]
45. Meng, F.; Liu, Q.; Kim, R.; Wang, J.; Liu, G.; Ghahreman, A. Selective recovery of valuable metals from industrial waste lithium-ion batteries using citric acid under reductive conditions: Leaching optimization and kinetic analysis. *Hydrometallurgy* **2020**, *191*, 105160. [[CrossRef](#)]
46. Li, L.; Lu, J.; Zhai, L.; Zhang, X.; Curtiss, L.; Jin, Y.; Wu, F.; Chen, R.; Amine, K. A facile recovery process for cathodes from spent lithium iron phosphate batteries by using oxalic acid. *CSEE J. Power Energy Syst.* **2018**, *4*, 219–225. [[CrossRef](#)]
47. Verma, A.; Johnson, G.H.; Corbin, D.R.; Shiflett, M.B. Separation of Lithium and Cobalt from LiCoO₂: A Unique Critical Metals Recovery Process Utilizing Oxalate Chemistry. *ACS Sustain. Chem. Eng.* **2020**, *8*, 6100–6108. [[CrossRef](#)]
48. Nayaka, G.P.; Pai, K.; Santhosh, G.; Manjanna, J. Dissolution of cathode active material of spent Li-ion batteries using tartaric acid and ascorbic acid mixture to recover Co. *Hydrometallurgy* **2016**, *161*, 54–57. [[CrossRef](#)]
49. He, L.-P.; Sun, S.Y.; Mu, Y.Y.; Song, X.F.; Yu, J.G. Recovery of Lithium, Nickel, Cobalt, and Manganese from Spent Lithium-Ion Batteries Using l-Tartaric Acid as a Leachant. *ACS Sustain. Chem. Eng.* **2017**, *5*, 714–721. [[CrossRef](#)]

50. Setiawan, H.; Petrus, H.T.B.M.; Perdana, I. Reaction kinetics modeling for lithium and cobalt recovery from spent lithium-ion batteries using acetic acid. *Int. J. Miner. Metall. Mater.* **2019**, *26*, 98–107. [[CrossRef](#)]
51. Golmohammadzadeh, R.; Rashchi, F.; Vahidi, E. Recovery of lithium and cobalt from spent lithium-ion batteries using organic acids: Process optimization and kinetic aspects. *Waste Manag.* **2017**, *64*, 244–254. [[CrossRef](#)]
52. Ning, P.; Meng, Q.; Dong, P.; Duan, J.; Xu, M.; Lin, Y.; Zhang, Y. Recycling of cathode material from spent lithium ion batteries using an ultrasound-assisted DL-malic acid leaching system. *Waste Manag.* **2020**, *103*, 52–60. [[CrossRef](#)]
53. Li, L.; Fan, E.; Guan, Y.; Zhang, X.; Xue, Q.; Wei, L.; Wu, F.; Chen, R. Sustainable Recovery of Cathode Materials from Spent Lithium-Ion Batteries Using Lactic Acid Leaching System. *ACS Sustain. Chem. Eng.* **2017**, *5*, 5224–5233. [[CrossRef](#)]
54. Gerold, E.; Luidold, S.; Antrekowitsch, H. Decomposition of hydrogen peroxide in selected organic acids. In Proceedings of the European Metallurgical Conference, Salzburg, Austria, 30 June–27 July 2021; pp. 1–13.
55. Gerold, E.; Lerchhammer, R.; Antrekowitsch, H. Parameter Study on the Recycling of LFP Cathode Material Using Hydrometallurgical Methods. *Metals* **2022**, *12*, 1706. [[CrossRef](#)]
56. Roy, J.J.; Cao, B.; Madhavi, S. A review on the recycling of spent lithium-ion batteries (LIBs) by the bioleaching approach. *Chemosphere* **2021**, *282*, 130944. [[CrossRef](#)]
57. Sethurajan, M.; Gaydardzhiev, S. Bioprocessing of spent lithium ion batteries for critical metals recovery—A review. *Resour. Conserv. Recycl.* **2021**, *165*, 105225. [[CrossRef](#)]
58. Do, M.P.; Jegan Roy, J.; Cao, B.; Srinivasan, M. Green Closed-Loop Cathode Regeneration from Spent NMC-Based Lithium-Ion Batteries through Bioleaching. *ACS Sustain. Chem. Eng.* **2022**, *10*, 2634–2644. [[CrossRef](#)]
59. Bahaloo-Horeh, N.; Mousavi, S.M. Enhanced recovery of valuable metals from spent lithium-ion batteries through optimization of organic acids produced by *Aspergillus niger*. *Waste Manag.* **2017**, *60*, 666–679. [[CrossRef](#)]
60. Horeh, N.B.; Mousavi, S.M.; Shojaosadati, S.A. Bioleaching of valuable metals from spent lithium-ion mobile phone batteries using *Aspergillus niger*. *J. Power Sources* **2016**, *320*, 257–266. [[CrossRef](#)]
61. Wang, Y.; Xu, Z.; Zhang, X.; Yang, E.; Tu, Y. A green process to recover valuable metals from the spent ternary lithium-ion batteries. *Sep. Purif. Technol.* **2022**, *299*, 121782. [[CrossRef](#)]
62. Sidiq, A.L.; Floweri, O.; Karunawan, J.; Abdillah, O.B.; Santosa, S.P.; Iskandar, F. NCM cathode active materials reproduced from end-of-life Li-ion batteries using a simple and green hydrometallurgical recycling process. *Mater. Res. Bull.* **2022**, *153*, 111901. [[CrossRef](#)]
63. Liang, Z.; Ding, X.; Cai, C.; Peng, G.; Hu, J.; Yang, X.; Chen, S.; Liu, L.; Hou, H.; Liang, S.; et al. Acetate acid and glucose assisted subcritical reaction for metal recovery from spent lithium ion batteries. *J. Clean. Prod.* **2022**, *369*, 133281. [[CrossRef](#)]
64. Chen, X.; Fan, B.; Xu, L.; Zhou, T.; Kong, J. An atom-economic process for the recovery of high value-added metals from spent lithium-ion batteries. *J. Clean. Prod.* **2016**, *112*, 3562–3570. [[CrossRef](#)]
65. Yao, L.; Xi, Y.; Han, H.; Li, W.; Wang, C.; Feng, Y. LiMn₂O₄ prepared from waste lithium ion batteries through sol-gel process. *J. Alloys Compd.* **2021**, *868*, 159222. [[CrossRef](#)]
66. Singh, O.V.; Kumar, R. Biotechnological production of gluconic acid: Future implications. *Appl. Microbiol. Biotechnol.* **2007**, *75*, 713–722. [[CrossRef](#)]
67. Wong, C.M.; Wong, K.H.; Chen, X.D. Glucose oxidase: Natural occurrence, function, properties and industrial applications. *Appl. Microbiol. Biotechnol.* **2008**, *78*, 927–938. [[CrossRef](#)]
68. Bankar, S.B.; Bule, M.V.; Singhal, R.S.; Ananthanarayan, L. Glucose oxidase—An overview. *Biotechnol. Adv.* **2009**, *27*, 489–501. [[CrossRef](#)]
69. Li, C.; Lin, J.; Gao, L.; Lin, H.; Lin, J. Modeling and simulation of enzymatic gluconic acid production using immobilized enzyme and CSTR-PFTR circulation reaction system. *Biotechnol. Lett.* **2018**, *40*, 649–657. [[CrossRef](#)]
70. Anastassiadis, S.; Morgunov, I.G. Gluconic acid production. *Recent Pat. Biotechnol.* **2007**, *1*, 167–180. [[CrossRef](#)] [[PubMed](#)]
71. Antonick, P.J.; Hu, Z.; Fujita, Y.; Reed, D.W.; Das, G.; Wu, L.; Shivaramaiah, R.; Kim, P.; Eslamimanesh, A.; Riman, R.E. Bio- and mineral acid leaching of rare earth elements from synthetic phosphogypsum. *J. Chem. Thermodyn.* **2019**, *132*, 491–496. [[CrossRef](#)]
72. Mouna, H.M.; Baral, S.S. A bio-hydrometallurgical approach towards leaching of lanthanum from the spent fluid catalytic cracking catalyst using *Aspergillus niger*. *Hydrometallurgy* **2019**, *184*, 175–182.
73. Naseri, T.; Mousavi, S.M.; Kuchta, K. Environmentally sustainable and cost-effective recycling of Mn-rich Li-ion cells waste: Effect of carbon sources on the leaching efficiency of metals using fungal metabolites. *Waste Manag.* **2023**, *157*, 47–59. [[CrossRef](#)]
74. Liu, Q.; Bai, J.F.; Gu, W.H.; Peng, S.J.; Wang, L.C.; Wang, J.W.; Li, H.X. Leaching of copper from waste printed circuit boards using *Phanerochaete chrysosporium* fungi. *Hydrometallurgy* **2020**, *196*, 105427. [[CrossRef](#)]
75. Rasoulnia, P.; Hajdu-Rahkama, R.; Puhakka, J.A. High-rate and-yield continuous fluidized-bed bioconversion of glucose-to-gluconic acid for enhanced metal leaching. *Chem. Eng. J.* **2023**, *462*, 142088. [[CrossRef](#)]
76. Roshanfar, M.; Golmohammadzadeh, R.; Rashchi, F. An environmentally friendly method for recovery of lithium and cobalt from spent lithium-ion batteries using gluconic and lactic acids. *J. Environ. Chem. Eng.* **2019**, *7*, 102794. [[CrossRef](#)]
77. Fan, E.; Shi, P.; Zhang, X.; Lin, J.; Wu, F.; Li, L.; Chen, R. Glucose oxidase-based biocatalytic acid-leaching process for recovering valuable metals from spent lithium-ion batteries. *Waste Manag.* **2020**, *114*, 166–173. [[CrossRef](#)]

78. Gerold, E.; Antrekowitsch, H. Potenzialabschätzung von Synergieeffekten zur simultanen Rückgewinnung von Wertmetallen aus komplexen, metallhaltigen Reststoffen. *Osterr. Wasser-Abfallwirtsch.* **2022**, *74*, 22–31. [[CrossRef](#)]
79. Tao, R.; Xing, P.; Li, H.; Cun, Z.; Wang, C.; Ma, S.; Sun, Z. Kinetics study and recycling strategies in different stages of full-component pyrolysis of spent LiNi_xCo_yMn_zO₂ lithium-ion batteries. *Waste Manag.* **2023**, *155*, 8–18. [[CrossRef](#)]

Disclaimer/Publisher's Note: The statements, opinions and data contained in all publications are solely those of the individual author(s) and contributor(s) and not of MDPI and/or the editor(s). MDPI and/or the editor(s) disclaim responsibility for any injury to people or property resulting from any ideas, methods, instructions or products referred to in the content.